Stability of Highly Inclined Boreholes

B.S. Aadnoy, SPE, Rogaland Regional C.
M.E. Chenevert, SPE, U. of Texas

Summary. Hole inclination produces alterations in the stress state around the borehole and in the physical properties of the rock. Depending on specific conditions, such effects may lead to collapse of the borehole or a reduction in the fracture-initiation pressure. This paper shows how to determine such effects through the application of stress analysis and rock mechanics.

Introduction

Stability of deviated boreholes is an important subject. Such problems as lost circulation may create hazardous conditions, while borehole collapse often results in enlargement of the borehole, causing numerous problems—e.g., poor cement displacement. The problems may exist in the producing phase of a borehole, as well as when drilling.

This paper is based on a linear elastic and isotropic model for stresses around the wellbore, with the aim of trying to understand the general behavior of inclined boreholes. The model is first used to study the two fracturing mechanisms. It was found that borehole collapse is caused mainly by shear but also by tensile failure, while fracturing of the wellbore is caused predominantly by tensile failure. Furthermore, when the wellbore is rotated from a vertical to a horizontal position, the analysis shows that the borehole becomes more sensitive toward collapse. For laminated sedimentary rocks, a weakness plane may subject the well toward collapse for hole angles between 10 and 40° [0.17 and 0.7 rad]. In tectonically stressed areas, the collapse stability may be improved by choosing the proper geographic direction for the borehole. The fracturing gradient generally decreases with increased borehole inclination. A simple formula is included to estimate the fracture initiation gradients for inclined holes if data for a vertical hole are known.

The input data to the analysis are composite curves from the U.S. gulf coast area. We believe, however, that the results obtained may be applicable to any continuous depositional basin.

Borehole stability is currently being given considerable attention in Norway. With a number of offshore fields under planning and development, a substantial saving in expenditures is envisioned if a field can be drained from three platforms instead of four. This can be realized by the application of extended-reach drilling methods. An increased borehole angle, however, brings about new problems. Cuttings transport, casing setting and cementing, and drillstring friction are examples of difficulties encountered in highly deviated boreholes. Also, the formation fracturing gradient decreases with increased borehole angle. With an increased application of oil-based muds, the prediction of the fracturing gradients becomes more important than ever. Here, fracturing must be avoided during the drilling phase, and the problem is to determine the maximum values for the formation-integrity tests.

Methods to predict fracturing gradients are typically based on empirical correlations between fracturing data, overburden data, and depth. Different methods of this nature are given in Refs. 1 through 7. Daines'[7] method in particular has been successfully applied in Norway by several oil companies. All these methods work for vertical wells. Only Bradley[8] studied the effect of borehole inclination on the fracturing gradient. The basic difference is that while the former (Refs. 1 through 7) used empirical correlations, Bradley used equations for the stresses around the borehole. In this paper, we will continue Bradley's approach because the study of stresses around the borehole also gives us a tool to study the failure mechanisms.

Before proceeding further, we will define some of the assumptions used here. In addition to using a linear-elastic and isotropic rock model for plane-strain conditions, we assume formations where all in-situ stresses are principal and directed horizontally and vertically, respectively. Generally, no information is available regarding the relative values of the two horizontal in-situ stresses, so they are assumed equal. The key in the analysis is that when a well is drilled, the rock surrounding the hole must take the load that was previously taken by the removed rock. As a result, an increase in stress around the wall of the hole, a stress concentration, is produced. If the rock is not strong enough, the borehole will fail.

If the borehole pressure is increased too much, fracturing or splitting of the borehole will occur. Conversely, if the borehole pressure is lowered too much, the borehole will collapse because of shear failure. In this case, rock fragment will break off from the wall and fall into the wellbore. These situations are shown in Fig. 1. Finally, note that the given stress equations are valid for an intact borehole only. As soon as the borehole fails, the stress situation changes and the equations are no longer valid.

Qualitative Discussion of Mechanisms Causing Wellbore Instabilities

As stated, two main types of wellbore-stability problems occur—fracturing of the wellbore at high borehole pressure and borehole collapse at low pressure. Wellbore collapse caused by clay swelling will not be covered here.

Before we proceed further, note the peculiar characteristics of rocks. As opposed to metallic materials that have high tensile strengths, rocks will generally be very weak in tension. Bradley[8] assumes rocks to have zero tensile strength and uses zero effective stress as his criterion for tensile failure. The reasoning is that rocks often fail along old cracks or flaws. Such an assumption is often also used by others.

In this paper, we argue that the main mechanism causing wellbore failure when the wellbore is fractured is tensile failure of the rock. For borehole collapse cases, the failure may be caused partly by tensile effects, but will be caused mainly by shear effects. This idea is illustrated in Fig. 2 and will be quantitatively shown later. A typical fracturing of the wellbore in shallow wells (horizontal fracture) is shown in Fig. 2a, where the overburden is being lifted. The axial stress, σ_z, goes tensile, while the radial and tangential stresses remain in a compressive state. Shear effects occur between $(\sigma_\theta, \sigma_z)$, $(\sigma_\theta, \sigma_r)$, and (σ_r, σ_z) because of large stress differences. These shear stresses will merely aid the fracturing process caused by the axial stress going tensile. No rock pieces will be released because both the shear and tensile stresses cause the fractures to go predominantly radially outward from the borehole. The equations used in this paper are not valid for this case. Fig. 2b illustrates the fracturing of a deeper well, where a vertical fracture is produced. Here, the radial and axial stresses are compressive, while the tangential stress, σ_θ, goes tensile. Even if a rock piece should be released from the borehole wall, the high wellbore pressure would keep it in place in both cases.

A borehole collapse process is illustrated in Fig. 2c. This is a typical pressure-drawdown problem. In this case, both the axial and the tangential effective stresses are compressive, while the radial effective stress goes tensile. If linear elasticity theory is applied, the failure should occur exactly at the wellbore wall. It is visualized

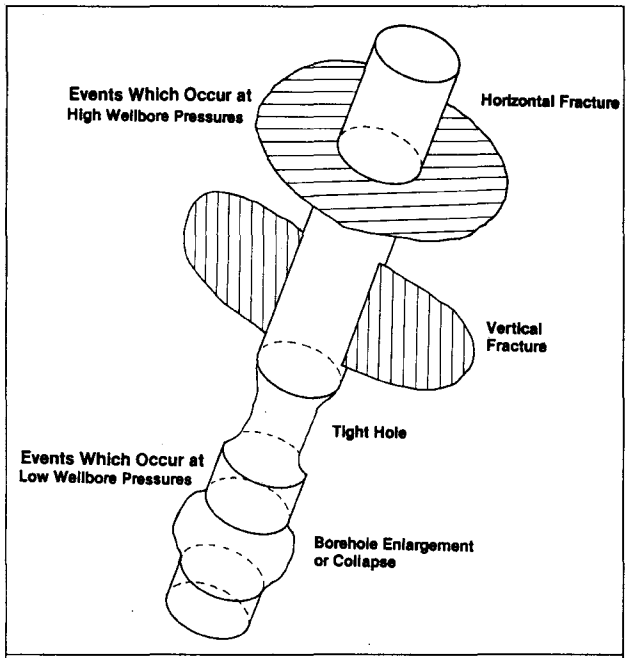

Fig. 1—Typical borehole problems.

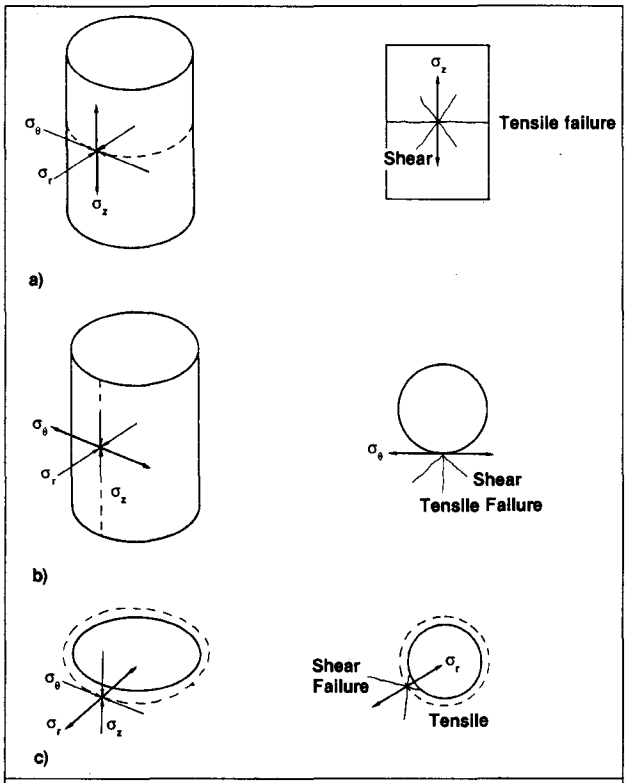

Fig. 2—Characteristic failures of boreholes: (a) horizontal fracture in shallow well, (b) vertical fracture in deep well, and (c) borehole collapse caused by shear with tensile radial stress.

that the wellbore sometimes fails in tension around a circumference as shown in Fig. 2c. In this case, the presence of radial failure aids the shear stresses in releasing pieces of rocks from the wellbore. If the wellbore pressure is lower than the formation pressure, the flow of formation fluids into the wellbore will wash the released pieces of rock into the wellbore.

Haimson and Herrick[9] have recently performed an experimental program studying borehole collapse. They conclude that the major

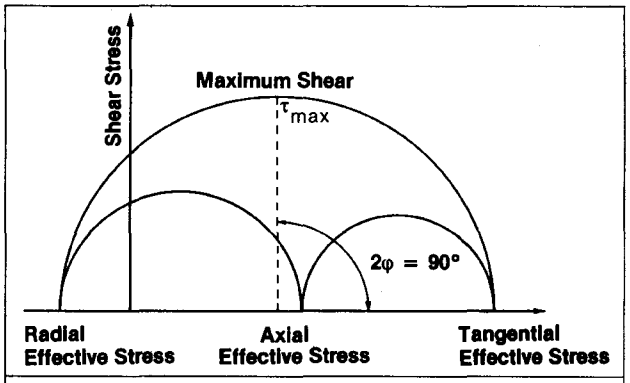

Fig. 3—Mohr's circle for collapse case.

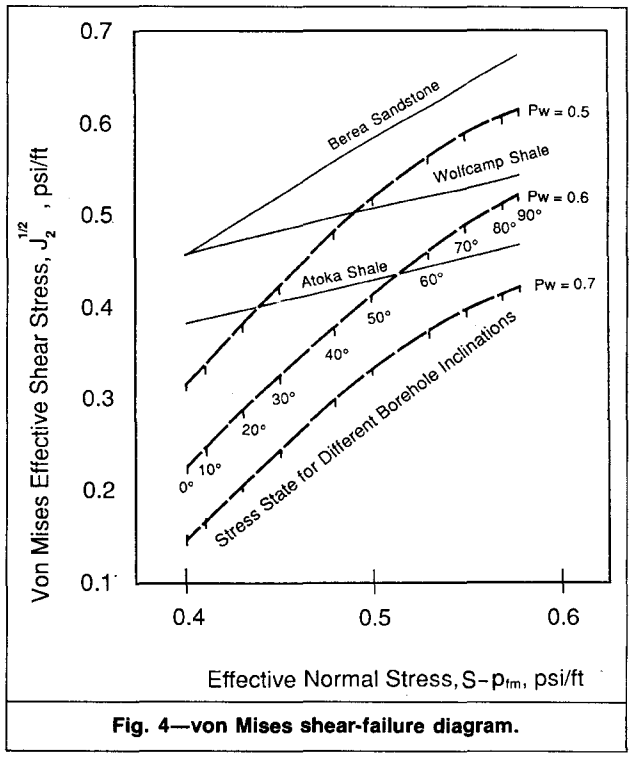

Fig. 4—von Mises shear-failure diagram.

breakout mechanism is apparently tensile rupture along surfaces to the borehole wall aided by shear failure in the radial direction. Also, they conclude that the collapse occurs at the position of the borehole that corresponds to the direction of the least in-situ stress normal to the axis of the hole. This is fully in line with our analysis.

Regarding the direction of the shear forces, for a vertical borehole under idealized conditions, the radial, tangential, and axial stresses become principal stresses. This means that no shear forces exist along the direction of these stresses. At an angle with respect to these stresses, however, shear forces will reach a maximum. A Mohr diagram is a convenient way to represent these shear stresses and their directions. Fig. 3 is a three-dimensional Mohr diagram for the borehole-collapse case. The shear stress reaches a maximum at point τ_{max}. This corresponds to an angle of $\alpha=45°$ [0.79 rad] from the radial and tangential axes, and the failure envelope approaches the Mohr circle at an angle of 30 to 45° [0.52 to 0.79 rad]. Spalling of the wellbore often results in concoidal-shaped rock fragments. Closer inspection of these shows that the shear failure often starts out at about a 30 to 45° [0.52- to 0.79-rad] angle, as previously defined.

Shear Failure

Two obvious mechanisms causing borehole failure are shear and tensile failure. Many shear-failure theories have been proposed

TABLE 1—EFFECTIVE OCTAHEDRAL SHEAR STRESS AND EFFECTIVE NORMAL STRESS AS FUNCTIONS OF BOREHOLE ANGLE AND WELLBORE PRESSURE, FOR $\sigma_x = \sigma_y = 0.80$ psi/ft, $\sigma_z = 1.0$ psi/ft, and $p_{fm} = 0.46$ psi/ft

Borehole Angle, γ (degrees)	Effective Normal Stress (psi/ft)	Effective Octahedral Shear Stress (psi/ft)		
		$p_w = 0.50$ psi/ft	$p_w = 0.60$ psi/ft	$p_w = 0.70$ psi/ft
0	0.40	0.32	0.23	0.15
10	0.41	0.33	0.25	0.17
20	0.43	0.37	0.28	0.21
30	0.45	0.42	0.33	0.25
40	0.48	0.47	0.38	0.30
50	0.50	0.52	0.42	0.34
60	0.53	0.56	0.46	0.37
70	0.55	0.59	0.49	0.40
80	0.57	0.60	0.51	0.41
90	0.58	0.61	0.52	0.42

throughout the years, but it is well known that no single theory is satisfactory for all materials. Shear (compressive) failure will be discussed first, using the von Mises "three-principal-stress" criterion, then failure will be discussed, using the Mohr-Coulomb "two-principal-stress" criterion.

von Mises Yield Condition. One of the most-used failure theories is Mohr's hypothesis. In this hypothesis, however, only the largest and smallest principal stresses affect failure. According to Bradley,[8] more recent results have shown that the intermediate principal stress affects failure as well. The intermediate principal stress is included in stress studies by applying an extended von Mises yield criterion. All three principal stresses are taken into account. These failure criteria are given as

$$J_2^{1/2} = \sqrt{\tfrac{1}{6}[(\sigma_1-\sigma_2)^2+(\sigma_2-\sigma_3)^2+(\sigma_3-\sigma_1)^2]} \quad \ldots\ldots\ldots (1a)$$

and

$$S - p_{fm} = \tfrac{1}{3}(\sigma_1+\sigma_2+\sigma_3) - p_{fm}. \quad \ldots\ldots\ldots\ldots\ldots\ldots (1b)$$

Eq. 1a actually represents the second deviatoric stress invariant, which is then plotted in Fig. 4 vs. the first normal effective-stress invariant (Eq. 1b). It is therefore a model used to express the experimental data.

A typical failure envelope for three rocks based on the previous criteria is shown in Fig. 4. If the stress state of the rock element in question falls below a given rock-failure envelope, the borehole is stable with respect to shear. Conversely, a stress state above the failure envelope means that shear failure has occurred. Bradley[8] found that by plotting failure data vs. the average mean normal stress, a family of curves could be created.

TABLE 2—EFFECTIVE OCTAHEDRAL SHEAR STRENGTH AND EFFECTIVE NORMAL STRESS FOR VARIOUS ROCKS UNDER ELEVATED STRESS CONDITIONS[10,11]

σ_1 (psi/ft)	σ_2 (psi/ft)	σ_3 (psi/ft)	$J_2^{1/2}$ (psi/ft)	$S - p_{fm}$ (psi/ft)
Atoka Shale				
0.17	0.17	0.83	0.38	0.39
0.20	0.20	0.90	0.40	0.43
0.25	0.25	1.00	0.43	0.50
0.33	0.33	1.17	0.48	0.61
Berea				
0.13	0.13	0.92	0.46	0.40
0.17	0.17	1.15	0.57	0.49
0.18	0.18	1.26	0.62	0.54
0.20	0.20	1.38	0.68	0.59
Wolfcamp				
0.13	0.13	0.93	0.46	0.40
0.17	0.17	1.0	0.48	0.44
0.20	0.20	1.07	0.50	0.49
0.27	0.27	1.20	0.54	0.58

With the criteria given in Eq. 1 and the equations for stress around boreholes, a computer program was written to generate data for various wellbore orientations and rock-strength data. The equations used are given in the Appendix. First, the in-situ stresses are transformed to the direction of the borehole by Eq. A-3, then the stresses at the borehole wall are found with Eq. A-2. Finally, the principal stresses are calculated with Eq. A-4, and the shear and normal stresses acting on the rock are calculated with Eq. 1.

The horizontal in-situ stresses were held equal and the borehole direction was rotated from vertical to horizontal orientation. An example of the procedure follows. For a vertical well ($\gamma = 0°$ [0 rad]), the following values were assumed: $\sigma_{T1} = \sigma_{T2} = 0.8$ psi/ft [18 kPa/m], $\sigma_o = 1$ psi/ft [22.6 kPa/m], $p_{fm} = 0.46$ psi/ft [10.4 kPa/m], $\theta = 90°$ [1.57 rad] (see the Appendix for $\sigma_{max}/\sigma_{min}$ convention), and $p_w = 0.5$ psi/ft [11.3 kPa/m]. These are inserted into Eq. A-3 to get: $\sigma_x = \sigma_y = \sigma_{T1}$, $\sigma_{zz} = \sigma_o$, $\tau_{yz} = \tau_{xz} = \tau_{xy} = 0$. From Eq. A-2, we now obtain $\sigma_r = 0.5$ psi/ft [11.3 kPa/m], $\sigma_\theta = 1.1$ psi/ft [24.9 kPa/m], $\sigma_{zz} = 1$ psi/ft [22.6 kPa/m], and $\tau_{\theta z} = 0$. These in turn were used in Eq. A-4 to find the principal stresses, which become $\sigma_1 = 1.1$ psi/ft [24.9 kPa/m], $\sigma_2 = 1$ psi/ft [22.6 kPa/m], and $\sigma_3 = 0.5$ psi/ft [11.3 kPa/m]. Inserting these numbers into Eq. 1 we obtain $J_2^{1/2} = 0.321$ psi/ft [7.26 kPa/m] and $S - p_{fm} = 0.407$ psi/ft [9.2 kPa/m]. Repeating this procedure with $\gamma = 10°$ [0.17 rad], 20° [0.35 rad], etc., in Eq. A-3, the $p_w = 0.5$-psi/ft [11.3-kPa/m] curve of Fig. 4 can be constructed (see Table 1).

The same procedure was followed for $p_w = 0.6$ and 0.7 psi/ft [13.6 and 15.8 kPa/m]; such values are shown in Fig. 4. Note that increasing the wellbore pressure lowers the stress state away from the three rock-failure curves. This result is in agreement with field observations; increasing the mud weight often produces hole stability.

The rock-strength curves shown in Fig. 4 were developed with Eq. 1 and Llewelyn's[10] and Chenevert's[11] rock properties. For the purpose of displaying the effect of hole angle on the strength gradient of such rocks, it was assumed that the Berea sandstone, the Atoka shale, and the Wolfcamp shale all occurred at the same depth (15,000 ft [4570 m]). The reader should be cautioned not to use Fig. 4 in an all-inclusive manner, but rather to analyze a given rock by its specific stress conditions as encountered. Table 2 provides a listing of rock-strength conditions used in Fig. 4.

In the case of the Berea sandstone, the stress conditions were below the rock-failure curve for all values of wellbore pressure and hole angle. From this observation, it is concluded that this rock would be stable under all these conditions. For the case of the Atoka and Wolfcamp shales, the results were different. As shown, for $p_w = 0.5$ psi/ft [11.3 kPa/m], the Wolfcamp shale became unstable at an angle of about 45° [0.79 rad] and the Atoka at about 28° [0.49 rad]. For the higher wellbore pressures of $p_w = 0.7$ psi/ft [15.8 kPa/m], however, the wellbore was stable for all angles and for both shales.

The importance of increased wellbore pressure is obvious in Fig. 4. It should be pointed out that this effect does decrease the occurrence for shear failure; however, it also increases the occurrence

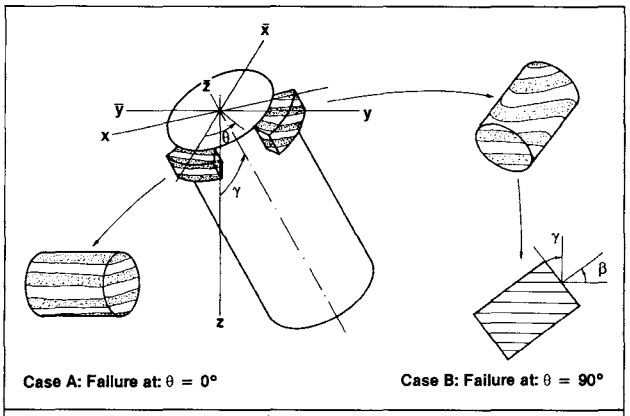

Fig. 5—Adaptation of core plug data to a real borehole.

for tensile (hydraulic fracturing) failure. So, in any given case, both shear and tensile failure must be studied. Tensile failure is discussed later in this paper.

Note that for the application of Eq. 1, maximum von Mises shear stress occurs in the direction of the least in-situ stress normal to the borehole axis. For equal horizontal in-situ stresses, this maximum will always be at the y axis ($\theta=90°$ [1.57 rad]). (For more detail, see Ref. 12.)

An interesting conclusion found in this study is that increasing the in-situ stresses with increased depth does not strongly affect the shear stress. This means that the well is not strongly sensitive to shear failure with increased depth.

Mohr-Coulomb Shear-Failure Model. The von Mises yield condition, as previously discussed, takes the intermediate principal stress into account. Now we will attempt to use the Mohr-Coulomb shear-failure model to study borehole collapse, which neglects the intermediate principal stress but does include the effect of the directional strengths of shales:

$$\tau=\tau_o+\sigma' \tan \alpha. \quad \ldots\ldots\ldots\ldots\ldots\ldots\ldots\ldots\ldots\ldots (2)$$

This model assumes that the total shearing resistance offered by an isotropic material to failure is the sum of the frictional resistance to slip along the potential failure plane and the cohesive strength, τ_o. σ' is the effective normal stress on the failure plane and tan α is the coefficient of internal friction. The shear and effective normal components of the stress acting on a plane inclined at an angle α with the direction of the maximum principal stress is

$$\sigma'=\tfrac{1}{2}(\sigma_1+\sigma_3)-\tfrac{1}{2}(\sigma_1-\sigma_3)\sin \alpha-p_{fm} \quad \ldots\ldots\ldots\ldots\ldots (3a)$$

and

$$\tau=\tfrac{1}{2}(\sigma_1-\sigma_3)\cos \alpha. \quad \ldots\ldots\ldots\ldots\ldots\ldots\ldots\ldots\ldots (3b)$$

The effective principal stresses are given as $\sigma'_k=\sigma_k-p_{fm}$, where $k=1,2,3$, and are usually used in most stress/failure representations (see Eq. A-5).

Jaeger[13] proposed an extension of the previous theory, in which the effects of the weakness planes are taken into account. This approach essentially establishes two Mohr-Coulomb envelopes, one applying to the material and the other describing failure along a weakness plane.

Chenevert and Gatlin[14] measured different rocks, varying the inclination of the bedding plane with respect to the maximum applied stress by use of "core plugs" cut from slabs of rock, and arrived at τ_o and tan α values as a function of bedding-plane orientation. To apply shear-failure data from core plugs, however, these data must be put into the proper context. It is already established by Haimson and Herrick[9] that the point of collapse is in the direction of the least in-situ stress.

In our case, the stresses with equal horizontal in-situ stress are always in the direction of the y axis ($\theta=90°$ [1.57 rad]). Even if the in-situ stresses are equal for a vertical hole, the stress along the x axis will gradually increase toward the weight of the overburden when the borehole is rotated toward horizontal position.

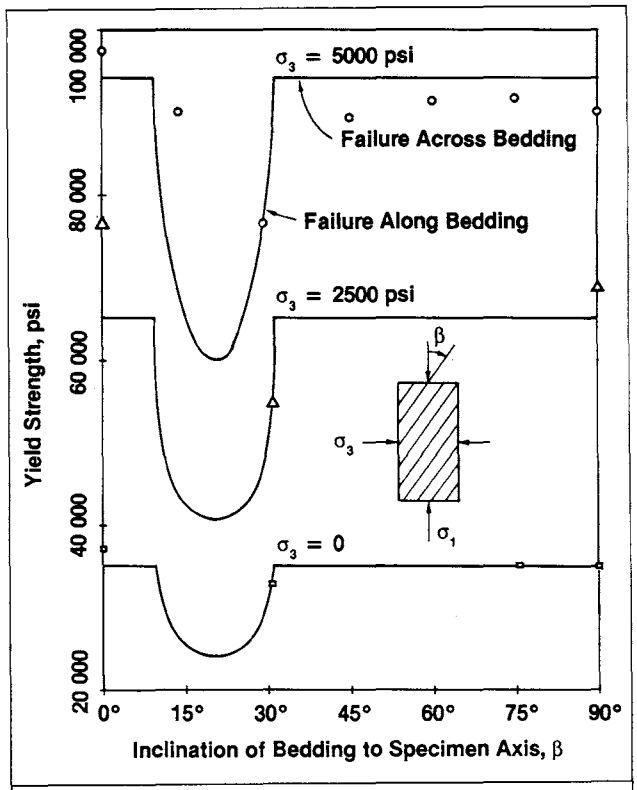

Fig. 6—Arkansas sandstone data vs. single weakness-plane theory.

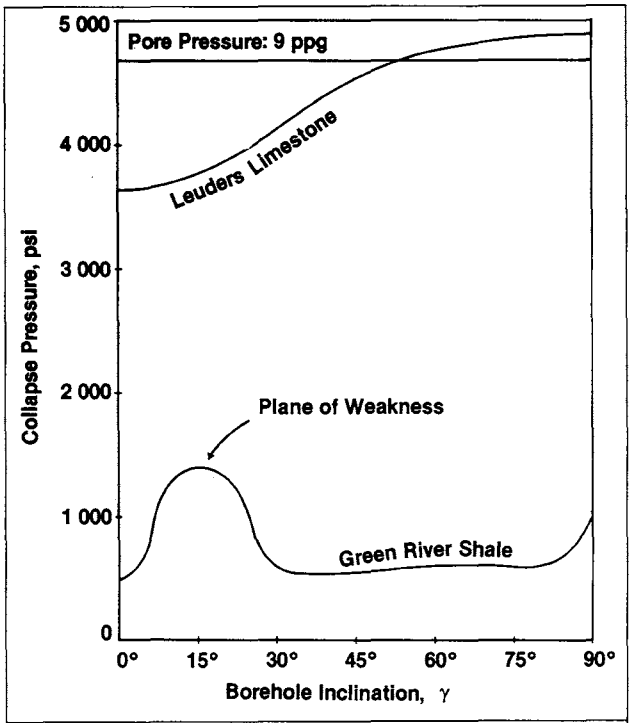

Fig. 7—Collapse pressure vs. borehole inclination at 10,000 ft.

Fig. 5 shows two elements on the borehole wall subjected to collapse. Actually, these "slices" are very thin, with very little curvature. The tangential (hoop) stress is definitely the largest, followed by the axial stress and the radial stress (the borehole pressure). In applying the coreplug data, the maximum applied stress corresponds to the hoop stress and the confining pressure to the borehole pressure. For our case, with equal horizontal in-situ stresses, the hole

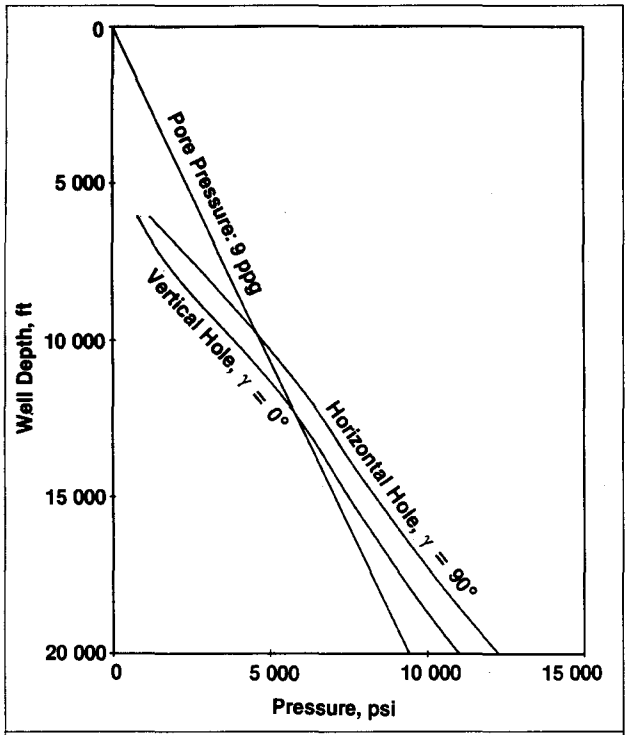

Fig. 8—Collapse pressure vs. depth for Leuders limestone.

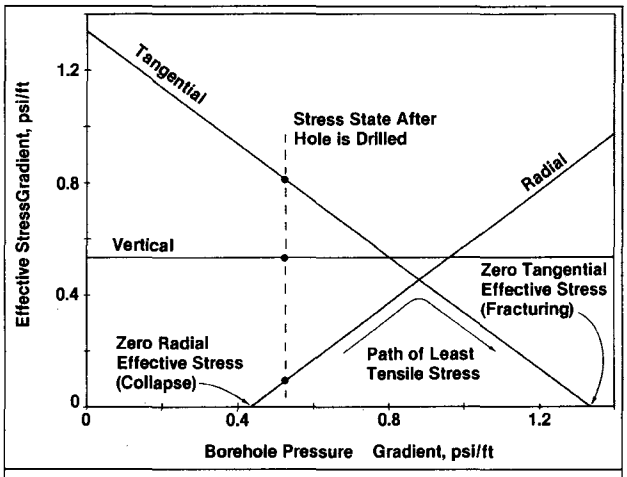

Fig. 9—Tensile stresses for deep vertical well.

will fail as in Case B of Fig. 5. Here we see that the directional shear strength comes into play. When core plugs are tested, the bedding plane is oriented at angle β with respect to the axially applied stress. We see that for Case B, the angle β corresponds to the borehole inclination γ. Fig. 5 and this part of the analysis is a simplified presentation. More details can be found in Ref. 12. In Fig. 6, the rock-yield-strength data are shown as a function of bedding-plane orientation. Clearly, the weakness plane is significant and reduces the shear strength of the rock by nearly a factor of two. We know in general that if the angle between the bedding plane and the applied axial load is in the range $10° < \beta < 40°$ [0.17 rad $< \beta <$ 0.7 rad], typically a sedimentary rock will exhibit a weakness plane (as seen in Fig. 6). It is therefore observed that the most sensitive range of inclination with respect to borehole collapse is $10° < \gamma < 40°$ [0.17 rad $< \gamma <$ 0.7 rad], because here the rock will fail along the bedding plane.

Let us for a moment consider a different case, namely a tectonically stressed case where one of the horizontal in-situ stresses is larger than the other. If this stress is in the y direction, the hole will collapse, as in Case A of Fig. 5. The interesting point here is that only one failure envelope applies for all borehole angles (as indicated in Fig. 5), and that the weakness plane does not come into play at all. In other words, inclining the borehole in the direction of the least in-situ stress forces any shear failure that may occur to cut across (rather than along) the bedding planes and therefore produces a very stable hole against collapse. Note that in the above analysis, we assumed that the hoop stress was a principal stress (a reasonable assumption). Inspection of Eq. A-4 shows that some shear effects arise that may adjust the direction of the principal stresses somewhat. This is neglected here.

Eqs. 2 and 3 were coupled with the mathematical model for the borehole and then used with Chenevert and Gatlin's[14] directional shear data and Eaton's[2] in-situ stresses. An example case is shown in Fig. 7. This curve shows the effect of hole angle on the collapse strength of the rock or the lowest permissible borehole pressure. The upper curve assumes normal pore pressure for a porous isotropic Leuder's limestone. For hole angles of $\gamma = 0$ to 50° [0 to 0.87 rad], a certain reduction in borehole pressure is permissible, but at an angle of $\gamma = 54°$ [0.94 rad], the hole will collapse in shear if the borehole pressure is equal to the initial pore pressure. For higher borehole angles, the hole will collapse if drilled in balance. This rock is nearly isotropic and has no weakness planes. It is clearly seen that for weak rocks, however, collapse of high-angle holes is a strong possibility, and similar behavior of real wells is actually reported from the North Sea. The values for Leuder limestone shown in Fig. 7 were developed as shown in the following example.

Assume we have the following data at 10,000 ft [3050 m]: $\sigma_o = 0.95$ psi/ft [21.5 kPa/m], $\sigma_{T1} = \sigma_{T2} = 0.85$ psi/ft [19.2 kPa/m]. If the same procedures are followed as those used for Fig. 4 (use of Eqs. A-3, A-2, and A-4), the principal stresses at 10,000 ft [3050 m] become $\sigma_1 = 17{,}000$ psi [117 MPa] $- p_w$, $\sigma_2 = 9{,}500$ psi [65.5 MPa], and $\sigma_3 = p_w$ for a vertical hole ($\gamma = 0°$ [0 rad]). From Chenevert and Gatlin,[14] the failure parameters for Eq. 2 are $\tau_o = 2{,}500$ psi [17.2 MPa] and $\alpha = 35°$ [0.61 rad]. Inserting the principal stresses and a pore pressure equal to p_w into Eq. 3, then these results into Eq. 2, together with the failure parameters τ_o and α, the left and right sides of Eq. 2 are satisfied for $p_w = 3{,}690$ psi [25.4 MPa]. This value is shown for $\gamma = 0°$ [0 rad] in Fig. 7. Note that for collapse pressures below the initial pore pressure, the mudcake has no effect, because fluids can freely flow from the formation into the wellbore. Therefore, we must set $p_{fm} = p_w$ when solving the above equations. Finally, if the previous procedure is repeated by inserting $\gamma = 10°$, 20° [0.17 rad, 0.35 rad], etc., in Eq. A-3, the complete upper curve of Fig. 7 is constructed.

The lower curve of Fig. 7 shows the same case for Green River shale, which has directional shear strengths and a clear weak zone in the neighborhood of $\gamma = 15°$ [0.26 rad], where the weakness plane comes into play. We have assumed that this shale is impermeable, keeping the pore pressure constant inside the rock. Also, it is much stronger than the limestone. Values for this curve were determined as in the previous example, except for different shear-strength data (Ref. 14).

Fig. 8 shows the collapse pressure vs. depth for Leuder's limestone, using the same two data sets as previously described. Two curves are given, one for the collapse of a horizontal hole ($\gamma = 90°$ [1.57 rad]) and one for a vertical hole ($\gamma = 0°$ [0 rad]). It is again seen that the collapse pressure increases with borehole angle. Also, it is observed that the well becomes more sensitive toward collapse with depth. In fact, at 12,000 ft [3660 m], for the vertical hole ($\gamma = 0°$ [0 rad]), the collapse pressure is equal to the pore pressure.

Evaluating Fig. 8, we see that at deeper depths—e.g., 20,000 ft [6100 m], the borehole will collapse at a borehole pressure considerably above the pore pressure. On the basis of deep-drilling experience, one can question whether this is true. Probably, there are elastoplastic effects present in a real borehole, as well as anisotropic effects that are not taken into account here. We believe, however, that some qualitative information can be deduced from this analysis. The borehole becomes more susceptible toward collapse the greater the inclination. Also, it is more likely to collapse at greater depth because of the increase of the general stress field. If the rock is laminated, it typically has a weakness plane, which gives the borehole high sensitivity toward collapse for borehole inclinations between 10 and 40° [0.17 and 0.7 rad].

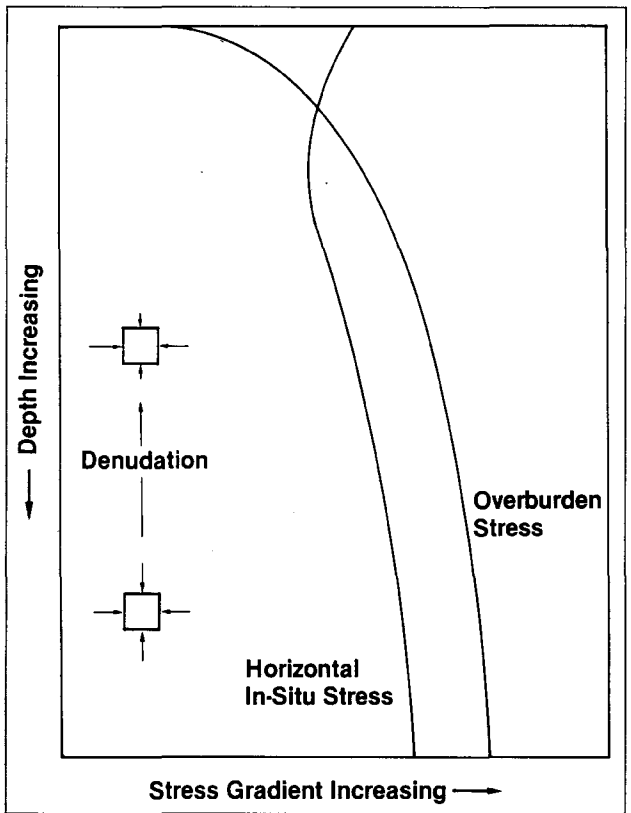

Fig. 10—Vertical and horizontal stress gradients vs. depth.

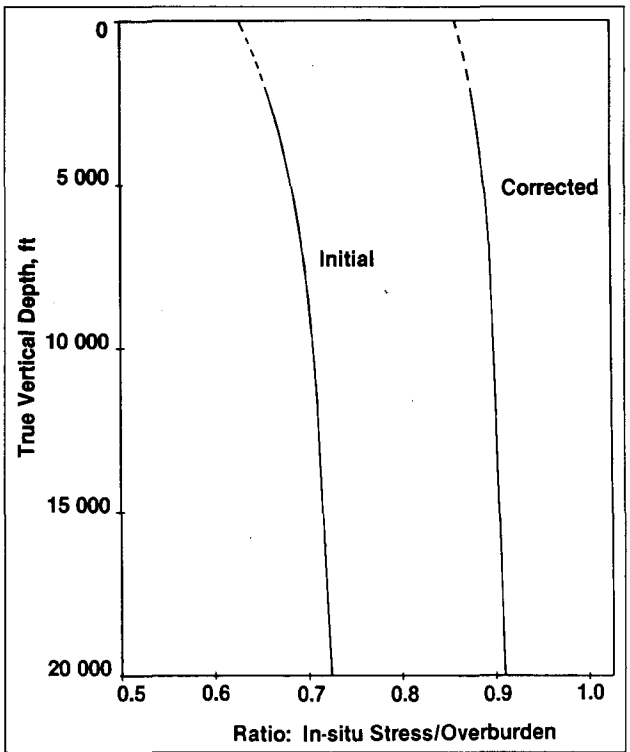

Fig. 11—Ratio horizontal/overburden stress vs. depth.

For cases with high tectonic in-situ stress in one direction, the borehole may be made very stable toward collapse by inclining it in the direction of the least in-situ stress. Here one failure envelope applies for all inclinations as shown in Case A of Fig. 5. On the other hand, inclining the borehole in the direction of maximum horizontal in-situ stress gives conditions for the weakness plane to apply, with resultant collapse problems between 10 and 40° [0.17- and 0.7-rad] inclination.

We believe that the weakness plane is a real effect, but possibly the Mohr-Coulomb criterion is too harsh with depth. The simulations also showed us that the weak chalks apparently are most sensitive toward collapse followed by the shales, and that the sandstones are the strongest rocks.

Tensile Failure

Tensile failure occurs when the least effective principal stress exceeds the rock tensile strength (see Eq. A-5) for a definition of principal stresses):

$$\sigma_{gr}-p_{fm}\leq\sigma_{\text{tensile}}. \quad \ldots\ldots\ldots\ldots\ldots\ldots\ldots\ldots\ldots\ldots\ldots\ldots\ldots\ldots (4)$$

Bradley[8] argues, and we agree, that the tensile strength of the rock is zero, because it is assumed that a fracture initiates in a flaw, joint, or existing fracture. Tensile failure of the rock is the most important failure mechanism of a wellbore because the rock is so weak in tension. We use Bradley's definition here. To illustrate the mechanisms of borehole failures, consider the following example.

As a well may be subjected to fracturing pressures, as well as drawdown pressures, a complete model should take into account both extremes. Assume a deep vertical well with equal in-situ stresses of 0.9 psi/ft [20.4 kPa/m] and an overburden gradient of 1 psi/ft [22.6 kPa/m]. The pore-pressure gradient is assumed to be 0.465 psi/ft [10.5 kPa/m]. Eqs. A-3, A-2, and A-4 for principal stresses at the wellbore will then reduce to the following, if we apply the effective-stress concept from Eq. A-5.

For radial effective stress,

$$\sigma_1'=\sigma_r-p_{fm}=p_w-0.465; \quad \ldots\ldots\ldots\ldots\ldots\ldots\ldots\ldots\ldots\ldots (5a)$$

for tangential effective stress,

$$\sigma_2'=\sigma_\theta-p_{fm}=2\sigma_{T1}-p_w-p_{fm}=1.335-p_w; \quad \ldots\ldots\ldots\ldots\ldots (5b)$$

and for vertical effective stress,

$$\sigma_3'=\sigma_z-p_{fm}=0.535. \quad \ldots\ldots\ldots\ldots\ldots\ldots\ldots\ldots\ldots\ldots\ldots\ldots (5c)$$

Because all shear terms vanish in this idealized case, Eqs. 5a through 5c all represent principal stresses. All these principal effective stresses are plotted in Fig. 9 as a function of the wellbore pressure. Three data points are plotted on these stress lines that reflect the state of stress at the borehole wall right after the well is drilled. By increasing the pressure in the borehole, p_w, we see that the vertical stress stays constant, the tangential stress goes down, and the radial stress increases. If the tangential stress reaches the zero value, as we have shown for $p_w=1.3$ psi/ft [29.4 kPa/m], fracturing occurs.

To use the figure, note that the least effective principal stress is the critical value, and when any of the stresses go below the x axis, the rock goes into tension and fails.

Note that when the borehole pressure reaches that of the native formation fluids, the effective radial stress is zero (see Fig. 9 for $p_w=0.465$ psi/ft [10.5 kPa/m]). Therefore, we will claim that when the borehole pressure is equal to or lower than the formation pressure, the possibility for radial tensile failure exists.

If the borehole pressure is increased from such values, the radial stress is the least principal stress up to a value where the radial and tangential stresses are equal (see Fig. 9 for $p_w=0.9$ psi/ft [20.4 kPa/m]). At this point, the borehole has maximum stability and the stress state is equal to that for the virgin formation. By increasing the wellbore pressure beyond this point, the stability of the wellbore gradually decreases; however, note that the tangential stress is now the least principal stress. Finally, when the failure curve is reached, the tangential stress goes tensile and a vertical fracture occurs.

Borehole collapse is defined as a shear failure. Fig. 9 at $p_w=0.435$ psi/ft [9.8 kPa/m] suggests that a tensile failure mode may exist simultaneously, as Haimson and Herrick[9] concluded. However, we use only the tensile failure as the failure mechanisms during fracturing.

This discussion explains the observed behavior of boreholes. When fracturing a wellbore, a fracture penetrating radially outward will be created. It is believed that this mechanism is mostly tensile, but the high shear stresses defined by Eq. 1 may accompany failure and possibly affect the direction of the fracture away from the borehole. When a borehole has collapsed, sometimes spalling has occurred. Here, concoidal-fracture pattern is often seen on the rock fragments brought up to the surface. This pattern is created by shear failure of the borehole wall. The rock fragments are then released from the borehole by a radially tensile failure.

Horizontal vs. Vertical Fractures

The field of petroleum engineering is concerned mostly with deep wells. There are cases, however, where shallow-well behavior is important.

The stress equations do not explain why horizontal fractures form above about 2,000 ft [610 m], while at greater depths, vertical fractures form, as given by Schechter.[15] The answer may be given by Jamison and Cook[16] and Brown,[17] who report that the horizontal in-situ stresses near the surface often exceed the overburden weight. They conclude that this may be a result of movement of crustal plates, plastic yield and subsequent elastic deformation on unloading during partial denudation, creep under sustained loads on geologic time scale, topography, tectonic forces of often ill-defined origin, and a general contraction of the earth's crust. For example, imagine a piece of rock buried very deeply and subjected to high loads. When the surface erodes, the rock will be uncovered. The overburden weight has been reduced significantly, but the two horizontal in-situ stresses will remain basically the same as at greater depth. The effects described imply that horizontal fractures occur near the surface, because the horizontal in-situ stresses here often exceed the weight of the overburden.

Fracture Gradient for Deviated Boreholes

When a new field development is started, a number of vertical delineation wells are usually drilled. At this point, information about the wells and the field is limited. After finishing a well, one has some leakoff data available or lost-circulation information, overburden data, and pore-pressure information. Although limited, these data will be shown useful in predicting the fracture initiation gradients for inclined boreholes drilled in the same formation. In other words, using all available information from the early development stage, we can predict the expected behavior for the production drilling phase and for the life of the field. One assumption, however, is that the area of the delineation wells and the rest of the reservoir basically have the same properties. This paper studies wellbore fracture at the borehole wall only, which therefore provides information on fracture initiation and not fracture propagation.

Pore pressure can be obtained by direct measurements in sands or indirectly in shales by, for example, the *d*-exponent method. The overburden-weight curve is typically generated from density logs. Inspection of the stress equations (Eqs. A-2 and A-3) reveals that the only unknowns are the horizontal in-situ stresses, provided that the fracture gradient is known. Direct measurements of the in-situ stresses are not performed in deeper wells except for very special cases. Because the magnitudes of the horizontal in-situ stresses are absolutely necessary to apply the proposed method, they must be obtained by indirect means. To do so, we will first assume that the two horizontal in-situ stresses are equal. This is a common assumption for a relaxed continuous depositional basin, but not always true.

For a deeper vertical borehole, a vertical fracture will form, and as discussed earlier, the fracture pressure is a function of the tangential stress in Eq. 5 and the tensile failure criteria in Eq. 4. When fracture pressure is solved for the horizontal in-situ stresses, it becomes

$$\sigma_{T1}=\tfrac{1}{2}(p_{wf}+p_{fm}+\sigma_{\text{tensile}}+A), \quad \ldots\ldots\ldots\ldots\ldots\ldots (6)$$

where A is a correlation coefficient and $\sigma_{\text{tensile}}=0$, according to Eq. 4. Now the horizontal in-situ stresses can be estimated. We used fracture-gradient curves and an overburden-gradient curve from the U.S. gulf coast area derived by Eaton[2] and calculated the horizontal in-situ stresses using Eq. 6, assuming that $A=0$. The results of these calculations are shown in Fig. 10. The ratio of the horizontal in-situ stress over the weight of the overburden is shown in Fig. 11. This ratio is on the order of 70%, a rather low value. Diagrams compiled by Pilkington[5] show consistently higher values.

Next, we use this information to construct fracture-gradient diagrams for inclined boreholes. As an example, we arbitrarily want the gradient at a 20° [0.35-rad] inclination. First, we transform the in-situ stress field to the borehole orientation by Eq. A-3. Next, we calculate the stresses caused by the borehole itself with Eq. A-2. Because the horizontal in-situ stresses are assumed equal, we get a stress state that is independent of the calculated geographic direction or the azimuth. Finally, the principal stresses are formed from Eq. A-4. All this is done numerically, because combining all these equations is impractical, and to find the fracture gradient, an iterative routine must be used by gradually increasing the borehole pressure until Eq. 4 is satisfied. However, the angle around the borehole, θ, is also a variable, and we must find the critical value for this angle. Differentiating the principal stresses with respect to θ and setting the resultant equation equal to zero, the minimum principal stress is found at $\theta=0°$ [0 rad] for the case of equal horizontal in-situ stresses. Introducing this information into the previously defined equation and letting $A=0$, we have

$$p_{wf}=3\sigma_y-\sigma_x-p_{fm}. \quad \ldots\ldots\ldots\ldots\ldots\ldots\ldots\ldots (7)$$

Fracture gradients for all hole angles from vertical to horizontal position were computed with Eq. 7. The results are shown in Fig. 12.

Before proceeding further, let us look at the two diagrams shown in Figs. 11 and 12. First, from Fig. 11, we have already observed that the horizontal in-situ stress is remarkably low. A horizontal in-situ stress is expected to approach the overburden weight with depth, while here it approaches only 70%. Second, inspection of Fig. 12 reveals quite a spread in the fracture gradients at a given depth. In fact, the reduction of the fracturing gradient when the hole is rotated from a vertical to a horizontal position is more than 5 lbm/gal at 20,000 ft [600 kg/m^3 at 6100 m]. Clearly, this value is extreme. With insufficient good field data to back it up, field experience generally does not show such a large variation.

The case studied is for a normally pressurized formation. Also interpreted from this diagram is that horizontal holes are not stable above 4,800 ft [1460 m] when drilling in balance, a clearly wrong conclusion.

On the basis of the previous discussion, the conclusion is that this particular data set gives us too low values for the horizontal in-situ stresses and that an adjustment must be made through the correlation coefficient A in Eq. 6. Knowing that Eq. A-2 strictly cannot predict horizontal fractures at shallower depths, we adjust the surface fracturing gradient because more rigorous criteria are lacking. Simply, the solution of Eq. 7 will be forced to be stable at surface—i.e, a horizontal hole drilled in balance (mud pressure equals pore pressure) will be stable and not fracture. Choosing a value for A with the above condition resulted in a fracture-gradient diagram as in Fig. 13. The corrected horizontal in-situ stress in Eq. 6 was used, together with the failure criterion of Eq. 4 replaced by the correlation coefficient, A. Now the difference in fracture gradients for a vertical fracture and a horizontal hole is reduced from >5 to <2 lbm/gal [>600 to <240 kg/m^3]. The corrected horizontal in-situ line in Fig. 10 shows the adjusted in-situ stress curve, which now is on the order of 90% of the overburden weight, a more realistic value.

The procedure described was performed for all pore pressures up to 16 lbm/gal [1917 kg/m^3], and the correlation coefficient was found to be a linear function of the pore pressure:

$$k=0.8-0.048p_{fm}, \quad \ldots\ldots\ldots\ldots\ldots\ldots\ldots\ldots (8)$$

where k is in psi/ft and p_{fm} is in pounds per gallon.

The argument for introducing this correlation coefficient is simply to be able to put field data into a continuum-mechanics perspective. Stress measurements should be performed in the future to check whether the in-situ stresses actually correspond to the corrected curve in Fig. 11.

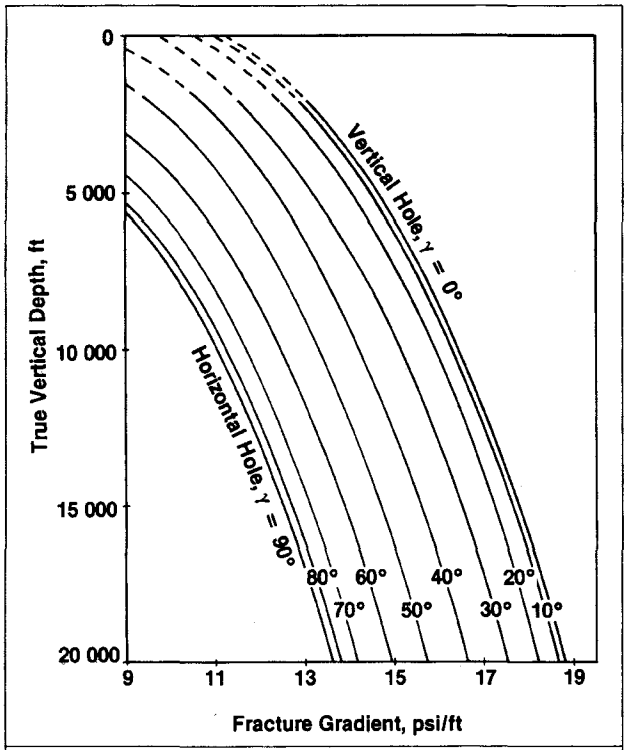

Fig. 12—Fracture gradients for deviated boreholes; normally pressurized formation (9 lbm/gal).

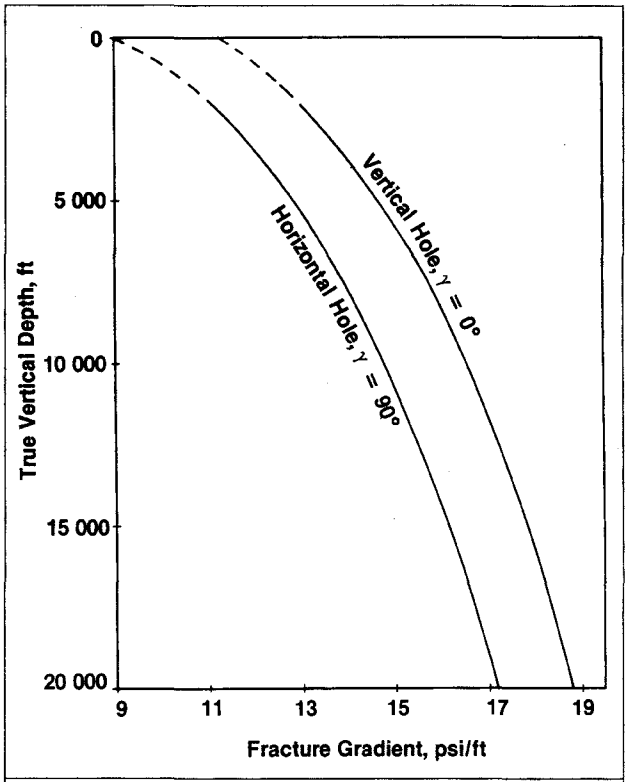

Fig. 13—Corrected fracture gradients for deviated boreholes; normally pressurized formation (9 lbm/gal).

We do not currently have a good understanding of this correlation coefficient, whether it represents such physical mechanisms as anisotropy or compensates for a systematic error in the input data. By constructing such diagrams as Fig. 13 for higher pore pressures, however, they all had the same parallel or bond characteristic. Therefore, we derived a simple equation for the fracture pressure per foot of depth for inclined boreholes:

$$p_{wf(\gamma)} = p^{o}_{wf} + \tfrac{1}{3}(p_o - 16)\sin^2 \gamma, \quad \ldots\ldots\ldots\ldots\ldots\ldots (9)$$

where $\sin^2 \gamma$ is in pounds per gallon. This equation is useful to predict the fracture-pressure gradient for inclined production wells. It only requires the vertical fracture gradient, the borehole inclination, and the pore pressure as input parameters. It is valid for pore pressures up to 16 lbm/gal [1917 kg/m^3].

Finally, Aadnoy[12] found that the shales typically have a high fracture gradient because they are nearly impermeable. If the rock is impermeable, the borehole pressure will not penetrate the rock and therefore will not aid in fracturing the rock inside the pores. Sands will accept some leakoff from the mud, thereby increasing the pore pressure inside the hole wall, which makes them weaker. This also suggests the importance of having a good-quality mudcake.

Conclusions

The two major types of borehole instability—borehole collapse and fracturing of the borehole—were studied for deviated boreholes by use of an ideal linear elastic and isotropic model. Input parameters used were Eaton's fracture data and overburden data for the U.S. gulf coast area and Chenevert's directional shear data. The objective was to derive quantitative criteria where possible, but also qualitative information regarding the behavior of inclined boreholes. To summarize, the following conclusions were reached.

Borehole collapse at low borehole pressures is caused by shear failure in combination with tensile failure. Generally, the deeper the well, the more likely the borehole is to become sensitive toward collapse. With the von Mises yield condition, it was found that increasing the borehole angle did not increase the sensitivity toward collapse. More trust was put into the study with the Mohr-Coulomb shear-failure theory, and Jaeger's weakness-plane theory. Here we found that the higher the borehole inclination, the more sensitive toward collapse the isotropic rocks become. For weak chalks, in particular, this may become a serious problem. For laminated rocks, the weakness plane makes the rock strongly sensitive toward collapse in the range of 10 to 40° [0.17- to 0.7-rad] inclination for a relaxed depositional basin. In a tectonically stressed region, on the other hand, the collapse stability can be improved by inclining the borehole in the same direction as the least in-situ stress. Our simulations also indicated that the weak chalks are most sensitive toward collapse, followed by the shales, and that the sandstones are the strongest rocks.

Fracturing of the borehole is mainly a tensile failure. In general, the fracturing gradient decreased with increased borehole inclination. A simple formula was derived with which the fracturing gradient could be estimated for any borehole angle, provided that the fracturing gradient for a vertical hole and the pore pressure are known. To arrive at these results, the horizontal in-situ stresses had to be adjusted with a correlation coefficient.

Fracturing of the borehole must be avoided, especially for oil-based muds. This equation therefore serves as a useful tool to estimate the value for the formation-integrity test. Finally, the shales are apparently the strongest rocks in the hole because they are nearly impermeable. This suggests that a very good mudcake should prevent lost circulation in a sandstone formation, as discussed by Hubbert and Willis.[4]

The occurrence of horizontal fractures at shallow depth is believed to be caused mainly by the horizontal stresses being larger than the weight of the overburden.

Future Work

As stated earlier, there is currently considerable interest in the borehole stability of deviated boreholes in Norway because of a number of offshore fields under development. The proposed fracturing-gradient model is currently being evaluated against older oil fields. We are also working on more advanced models, however, incorporating anisotropic rock behavior, possible plastic effects, and also taking into account the regional geology. Regarding borehole col-

lapse, a larger program is under way in Norway to determine rock properties and critical parameters experimentally. Also, a comprehensive numerical simulator developed by Aadnoy[12] takes anisotropic effects into account. The basic research is important to pursue. Application of the huge amounts of information available in the oil companies—information that is not currently adequately utilized and that forms the basis for the application of any theory—is as important.

Drilling and Logging Data. The mud logger on site compiles a large amount of data. These are routinely sent to the engineering department where some of them are used. However, a large portion are never organized, just stored somewhere. A more systematic analysis of all drilling and logging data definitely is needed.

Performing Leakoff Tests. All oil companies have their own procedures to follow when a leakoff test is performed. Typically, when pumping at a constant rate, the increase in pressure is recorded. The point at which the pressure vs. the cumulative pumped volume deviates from a straight line is typically taken as the leakoff point. Two main problems are associated with this type of test. First, the pressure chosen may not represent the true leakoff pressure. Second, experience shows that if two engineers run the same test, they may arrive at different leakoff pressures. Another problem arises because of lack of knowledge of mud properties. Mud gel strength and mud density are two such parameters. It may be necessary to run leakoff tests with bottomhole-pressure gauges in place to get accurate pressure values.

Two Fracturing-Gradient Diagrams. Most fracturing-gradient estimation methods found in the literature neglect to correlate with lithology. The casing points are usually found in competent shale sections and therefore represent the strong sections of the open hole. Lost circulation, on the other hand, often occurs in sands, which give lower fracturing gradients. Therefore, we suggest that two fracturing-gradient diagrams be developed, one for the shales and one for the sandstones or chalks.

Lost-Circulation and Collapse Information. Every time lost circulation is experienced or signs of borehole collapse are seen, efforts should be made to establish the wellbore pressure at the incident. This is valuable information when fracture and collapse diagrams for the borehole are constructed. Other relevant information—e.g., borehole inclination and lithology—should, of course, accompany the pressure data as input data to a borehole simulator. The direction of the collapse, for example, indicates the direction of the least in-situ stress. This type of information will provide valuable insight into the behavior of the borehole under the drilling phase, as well as the completion and production phases of the well.

Fracture Initiation and Propagation. The models used in this study are based on continuum-mechanics principles and define only the fracture-initiation pressure. The propagation of a fracture is a different problem and should be analyzed by fracture mechanics.

Once a fracture is initiated, it is believed that the pressure required to extend it corresponds to the least in-situ stress in the rock mass and the direction of the fracture may therefore shift as the fracture propagates away from the borehole. This paper makes no attempt to define crack-propagation-failure theory.

Nomenclature

a = constant used for wellbore radius
A,k = correlation coefficients
$J_2^{1/2}$ = deviatoric stress invariant (Eq. 1a), psi/ft [kPa/m]
p_{fm} = formation pressure per foot of depth, psi/ft [kPa/m]
p_w = wellbore pressure per foot of depth, psi/ft [kPa/m]
p^o_{wf} = fracturing pressure per foot of depth for vertical well, psi/ft [kPa/m]
$p_{wf}(\gamma)$ = fracturing pressure per foot of depth at any borehole angle, γ, psi/ft [kPa/m]
r = radius from borehole center
S = arithmetic average of three normal stresses, psi [kPa]
x = reference axis of coordinate system
α = angle
$\tan\alpha$ = rock coefficient of internal friction
β = angle between axial load and bedding plane during triaxial tests
γ = borehole deviation from vertical
δ_{ij} = Kronecker delta
θ = angular position around borehole
μ = Poisson's ratio, ~0.2 for most rocks (assumed)
σ' = effective normal stress per foot of depth, psi/ft [kPa/m]
σ_{gr} = rock grain stress per foot of depth, psi/ft [kPa/m]
σ_{ij} = total stresses
σ'_{ij} = effective stresses
σ_k = principal stress per foot of depth, psi/ft [kPa/m]
σ'_k = effective principal stress per foot of depth, psi/ft [kPa/m]
σ_o = overburden stress per foot of depth, psi/ft [kPa/m]
$\sigma_r,\sigma_\theta,\sigma_z$ = normal stress per foot of depth in cylindrical coordinates, psi/ft [kPa/m]
σ_{tensile} = tensile rock strength per foot of depth, psi/ft [kPa/m]
σ_{T1},σ_{T2} = horizontal in-situ stress per foot of depth, psi/ft [kPa/m]
$\sigma_x,\sigma_y,\sigma_{zz}$ = normal stress per foot of depth in rectangular coordinates (actually normal to and parallel to hole axis), psi/ft [kPa/m]
$\sigma_1,\sigma_2,\sigma_3$ = principal stress per foot of depth, psi/ft [kPa/m]
τ = shear stress, psi [kPa]
$\tau_{ij},\tau_{k\ell}$ = stress tensors, psi [kPa]
$\tau_{\max}$ = maximum shear stress, psi [kPa]
τ_o = cohesive rock strength, psi [kPa]
$\tau_{xy},\tau_{xz},\tau_{yz}$ = shear stress per foot of depth in rectangular coordinates, psi/ft [kPa/m]
$\tau_{\theta z}$ = shear stress per foot of depth in cylindrical coordinates, psi/ft [kPa/m]
ϕ = borehole azimuth angle from x axis

Superscripts

i,j,k,ℓ = tensor indices

Acknowledgments

We express appreciation to William B. Bradley and the many people who have supported and encouraged this work. Special thanks go to Rogaland U., Norway, and to the members of the Drilling Fluids Research Program at the U.of Texas—Chevron Oil Field Research Co., Conoco Inc., Shell Development Co., and Union Oil Co. of California—who provided the necessary time and financial support.

References

1. Matthews, W.R. and Kelley, J.: "How To Predict Formation Pressure and Fracture Gradient," *Oil & Gas J.* (Feb. 1967) 92-106.
2. Eaton, B.A.: "Fracture Gradient Prediction and Its Application in Oilfield Operations," *JPT* (Oct. 1969) 1353-60; *Trans.*, AIME, **246**.
3. Anderson, R.A., Ingram, D.S., and Zanier, A.M.: "Determining Fracture Pressure Gradients From Well Logs," *JPT* (Nov. 1973) 1259-68.
4. Hubbert, M.K. and Willis, D.G.: "Mechanics of Hydraulic Fracturing," *JPT* (June 1957) 153-68; *Trans.*, AIME, **210**.
5. Pilkington, P.E.: "Fracture Gradient Estimates in Tertiary Basins," *Pet. Eng. Intl.* (May 1978) 138-48.
6. Brennan, R.M. and Annis, M.R.: "A New Fracture Prediction Technique That Shows Good Results in the Gulf of Mexico Abnormal Pressure," paper SPE 13210 presented at the 1984 SPE Annual Technical Conference and Exhibition, Houston, Sept. 16-19.

7. Daines, S.R.: "Prediction of Fracture Pressures for Wildcat Wells," *JPT* (April 1982) 863-72.
8. Bradley, W.B.: "Failure of Inclined Boreholes," *J. Energy Res. Tech.* (Dec. 1979) 232-39;*Trans.*, AIME, **101**.
9. Haimson, B.C. and Herrick, C.G.: "Borehole Breakouts—a New Tool for Estimating In-Situ Stresses?," *Proc.*, Intl. Symposium on Rock Stress and Rock Stress Measurements, Stockholm (Sept. 1-3, 1986) 271-80.
10. Llewelyn, B.C.: "Compaction and Failure Studies on Texas Gulf Coast Geopressured Geothermal Sandstones and Shales," MS thesis, U. of Texas, Austin (May 1980).
11. Chenevert, M.E.: "Adsorptive Pore Pressures of Argillaceous Rocks," *Proc.*, 11th Symposium on Rock Mechanics, U. of California, Berkeley (June 1969) 599-627.
12. Aadnoy, B.S.: "Modeling of the Stability of Highly Inclined Boreholes in Anisotropic Rock Formations," paper SPE 16526 presented at the 1987 SPE Offshore Europe Conference, Aberdeen, Sept. 8-11.
13. Jaeger, J.C.: "Shear Failure of Anisotropic Rocks," *Geol. Mag.* (1960) **97**, 65-72.
14. Chenevert, M.E. and Gatlin, C.: "Mechanical Anisotropies of Laminated Sedimentary Rocks," *SPEJ* (March 1965) 67-77; *Trans.*, AIME, **234**.
15. Schechter, R.S.: *Advanced Production Notes*, U. of Texas Coop Bookstore, Austin (1984).
16. Jamison, D.B. and Cook, N.G.: "An Analysis of Measured Values for the State of Stress in the Earth's Crust," report LBL-7671, SAC-07, Earth Sciences Div., Lawrence Berkeley Laboratory and Dept. of Mineral Science and Mining Engineering, U. of California, Berkeley (Aug. 1978).
17. Brown, E.T. and Hoke, E.: "Trends in Relationships Between Measured In-Situ Stresses and Depth," technical note, *Intl. J. Rock Mech. Min. Sci. & Geomech. Abstr.* (Aug. 1978) **15**, 211-15.

Appendix

Stress Around a Borehole. The equations for stress around a borehole as a function of radial distance away from the wellbore are given. The model assumes linear elasticity and isotropic rock properties. The solution is based on plane-strain conditions. Derivations of the equations can be found in Refs. 9 and 10. Note that we define compressive stresses as positive.

$$\sigma_r=\tfrac{1}{2}(\sigma_x+\sigma_y)\left(1-\frac{a^2}{r^2}\right)+\tfrac{1}{2}(\sigma_x-\sigma_y)\left(1+3\frac{a^4}{r^4}-4\frac{a^2}{r^2}\right)\cos 2\theta$$

$$+\tau_{xy}\left(1+3\frac{a^4}{r^4}-4\frac{a^2}{r^2}\right)\sin 2\theta+\frac{a^2}{r^2}p_w. \quad \text{.....(A-1a)}$$

$$\sigma_\theta=\tfrac{1}{2}(\sigma_x+\sigma_y)\left(1+\frac{a^2}{r^2}\right)$$

$$-\tfrac{1}{2}(\sigma_x-\sigma_y)\left(1+3\frac{a^4}{r^4}\right)\cos 2\theta$$

$$-\tau_{xy}\left(1+3\frac{a^4}{r^4}\right)\sin 2\theta-\frac{a^2}{r^2}p_w. \quad \text{.....(A-1b)}$$

$$\sigma_z=\sigma_{zz}-2\nu(\sigma_x-\sigma_y)\frac{a^2}{r^2}\cos 2\theta-4\nu\tau_{xy}\frac{a^2}{r^2}\sin 2\theta. \quad \text{.....(A-1c)}$$

$$\tau_{r\theta}=[\tfrac{1}{2}(\sigma_x-\sigma_y)\sin 2\theta+\tau_{xy}\cos 2\theta]\left(1-3\frac{a^4}{r^4}+2\frac{a^2}{r^2}\right).$$

$$\text{.....(A-1d)}$$

$$\tau_{rz}=(\tau_{xz}\cos\theta+\tau_{yz}\sin\theta)\left(1-\frac{a^2}{r^2}\right). \quad \text{.....(A-1e)}$$

$$\tau_{\theta z}=(-\tau_{xz}\sin\theta+\tau_{yz}\cos\theta)\left(1+\frac{a^2}{r^2}\right). \quad \text{.....(A-1f)}$$

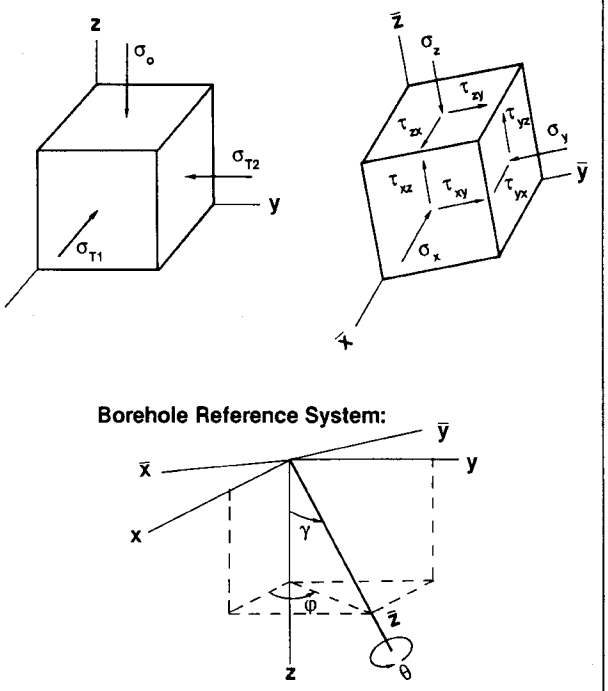

Fig. A-1—Coordinate transformations.

At the borehole, $r=a$, and these equations reduce to

$$\sigma_r=p_w, \quad \text{.....(A-2a)}$$

$$\sigma_\theta=(\sigma_x+\sigma_y-p_w)-2(\sigma_x-\sigma_y)\cos 2\theta-4\tau_{xy}\sin 2\theta, \quad \text{....(A-2b)}$$

$$\sigma_z=\sigma_{zz}-2\nu(\sigma_x-\sigma_y)\cos 2\theta-4\mu\tau_{xy}\sin 2\theta, \quad \text{.....(A-2c)}$$

$$\tau_{r\theta}=\tau_{rz}=0, \quad \text{.....(A-2d)}$$

and

$$\tau_{\theta z}=2(-\tau_{xz}\sin\theta+\tau_{yz}\cos\theta). \quad \text{.....(A-2e)}$$

Stresses When the Axis is Rotated. The principal in-situ stresses are transformed to the orientation of the borehole with the following tensor operator:

$$\tau_{ij}=\tau_{k\ell}\frac{\delta x^k}{\delta\bar{x}^i}\frac{\delta x^\ell}{\delta\bar{x}^j}.$$

The results of this transformation use the absolute angle between the respective axis. By introducing a set of reference angles, as shown in Fig. A-1, the above tensor can be transformed into the following set of equations:

$$\sigma_x=(\sigma_{T1}\cos^2\phi+\sigma_{T2}\sin^2\phi)\cos^2\gamma+\sigma_o\sin^2\gamma, \quad \text{....(A-3a)}$$

$$\sigma_y=(\sigma_{T1}\sin^2\phi+\sigma_{T2}\cos^2\phi), \quad \text{.....(A-3b)}$$

$$\sigma_{zz}=(\sigma_{T1}\cos^2\phi+\sigma_{T2}\sin^2\phi)\sin^2\gamma+\sigma_o\cos^2\gamma, \quad \text{...(A-3c)}$$

$$\tau_{yz}=0.5(\sigma_{T2}-\sigma_{T1})\sin(2\phi)\sin\gamma, \quad \text{.....(A-3d)}$$

$$\tau_{xz}=0.5(\sigma_{T1}\cos^2\phi+\sigma_{T2}\sin^2\phi-\sigma_o)\sin(2\gamma), \quad \ldots\ldots \text{(A-3e)}$$

and

$$\tau_{xy}=0.5(\sigma_{T2}-\sigma_{T1})\sin(2\phi)\cos^2\gamma. \quad \ldots\ldots\ldots\ldots\ldots\ldots \text{(A-3f)}$$

Here, the borehole deviation from vertical is defined as γ and the projected orientation with respect to the x axis is ϕ. (See Fig. A-1).

Principal Stresses. We are interested in the principal stresses, which are calculated as follows:

$$\sigma_1=\sigma_r=p_w \quad \ldots\ldots\ldots\ldots\ldots\ldots\ldots\ldots\ldots\ldots\ldots \text{(A-4a)}$$

and

$$\sigma_{2,3}=\tfrac{1}{2}(\sigma_\theta+\sigma_z)\pm\tfrac{1}{2}[(\sigma_\theta-\sigma_z)^2+4(\tau_{\theta z})^2]^{1/2}. \quad \ldots\ldots\ldots \text{(A-4b)}$$

After the principal stresses are calculated according to Eq. A-4, the subscripts are rearranged so that σ_1 is the largest and σ_3 is the smallest principal stress. This is necessary to use the Mohr-Coulomb theory properly.

Effective Stresses. When stresses in porous materials are considered, we usually assume the material to be a continuous medium. According to Terzaghi's effective-stress principle, we let the interparticle forces form effective stresses, which when added to the pore pressure, gives us the total stresses

$$\sigma_{ij}=(\sigma'_{ij}+\delta_{ij})p_{fm}, \quad \ldots\ldots\ldots\ldots\ldots\ldots\ldots\ldots\ldots\ldots\ldots \text{(A-5)}$$

where

σ_{ij} = total stresses in the ij direction,
σ'_{ij} = effective stresses in the ij direction,
p_{fm} = pore pressure, and
δ_{ij} = Kronecker delta.

Rigorous analysis shows that Eq. A-5 is a simplification for a compacted rock. For isotropic rocks, the Kronecker delta must be multiplied by a scaling factor, and for anisotropic rocks, each stress component has its own pore-pressure coefficient. Aadnoy[12] studied this in detail. For this analysis, however, we will assume that Eq. A-5 is sufficiently accurate.

SI Metric Conversion Factors

degrees	×	1.745 329	E−02	= rad
ft	×	3.048*	E−01	= m
lbm/gal	×	1.198 264	E+02	= kg/m^3
psi	×	6.894 757	E+00	= kPa
psi/ft	×	2.262 059	E+01	= kPa/m

*Conversion factor is exact.

SPEDE

Original SPE manuscript received for review March 15, 1987. Paper accepted for publication July 16, 1987. Revised manuscript received Sept. 11, 1987. Paper (SPE 16052) first presented at the 1987 SPE/IADC Drilling Conference held in New Orleans, March 15–18.

Discussion of Stability of Highly Inclined Boreholes

H. Simison, SPE, Bolland & Co.

I have read Aadnoy and Chenevert's paper, "Stability of Highly Inclined Boreholes" (Dec. 1987 *SPEDE*, Pages 364-74). I think they have made a major contribution to the understanding of highly inclined wellbore stability problems. While reading the paper, however, I found the following points that, in my opinion, merit corrective comments.

First, the fracture gradient scales in Figs. 12 and 13 (Page 371) in units of psi/ft are not correct according to the numerical values shown.

Second, the equation that predicts the fracture-pressure gradient for inclined wells (Eq. 9) is

$$p_{wf}(\gamma)=p^{\circ}_{wf}+\tfrac{1}{3}(p_o-16)\sin^2\gamma,$$

"where $\sin^2\gamma$ is in pounds per gallon."

I suppose the authors mean that the p_o (pore pressure) value must be put in Eq. 9 in units of pounds per gallon. If you do so, say for a horizontal well in a normal pressure formation (9 lbm/gal [1078 kg/m^3]), you obtain a numerical value of -2.33. To be consistent with the p_{wf} units used in the paper, the result of Eq. 9 must be in psi/ft. A corrective term of -2.33 psi/ft makes no sense.

Is the p_o value in lbm/gal? If this is the case, is there a conversion factor missing? Or are the p_{wf} units in Eq. 9 not psi/ft? I would appreciate the authors answering these questions.

SI Metric Conversion Factor

lbm/gal × 1.198 264 E+02 = kg/m^3

(SPE 18596) **SPEDE**

Authors' Reply to Discussion of Stability of Highly Inclined Boreholes

B.S. Aadnoy, SPE, Rogaland U.
M.E. Chenevert, SPE, U. of Texas

We thank Simison for his corrective comments. We will address each point.

1. The fracture gradient scale shown in Figs. 12 and 13 is erroneous. The correct scale is lbm/gal.

2. The sentence after Eq. 9 shall read: "where all pressures are in pounds per gallon." Any pressure unit can be used in Eq. 9 as long as it is consistent. Regrettably, the unit used in Eq. 9 is lbm/gal, which is not consistent with the units defined in the Nomenclature.

As an example, look at Fig. 13. At surface, the fracture gradient is about 11.3 lbm/gal [1354 kg/m^3] for a vertical hole, while a horizontal hole has a gradient of 9 lbm/gal [1078 kg/m^3]. The difference is about 2.3 lbm/gal [276 kg/m^3], as given by Eq. 9.

In addition to the points made by Simison, three errors have been found in the Appendix. The first paragraph of the Appendix refers the derivation of the equations to Refs. 9 and 10. This is not correct; these particular references were taken out of the reference list during the revision process.

In Eq. A-2c, the two last terms are both multiplied by Poisson's ratio, μ.

The squared term in the cosine expression in Eq. A-3f should read "cos γ."

We again thank Simison for his comments and hope that the above corrections will remove any misunderstanding in the application of our model.

(SPE 18736) **SPEDE**